Journal of Volcanology and Geothermal Research 455 (2024) 108197

Contents lists available at ScienceDirect

Journal of Volcanology and Geothermal Research

journal homepage: www.journals.elsevier.com/journal-of-volcanology-and-geothermal-research

Lava flow field development and lava tube formation during the 1858–1861 eruption of Vesuvius (Italy), unravelled by historical documentation, lidar data and 3D mapping

Thomas Lemaire [a,*], Daniele Morgavi [a], Paola Petrosino [a], Sonia Calvari [b], Leopoldo Repola [a], Lorenzo Esposito [a], Diego Di Martire [a], Vincenzo Morra [a], Francesco Frondini [c]

[a] Dept. of Earth, Environment and Resource Sciences (DiSTAR), University Federico II, Complesso Universitario di Monte Sant'Angelo, Via Vicinale Cupa Cintia 21, 80126 Napoli, Italy
[b] Istituto Nazionale di Geofisica e Vulcanologia, Osservatorio Etneo – Sezione di Catania, Piazza Roma 2, 95125 Catania, Italy
[c] Dept. of Physics and Geology, University of Perugia, piazza dell'Università 1, 06123 Perugia, Italy

ARTICLE INFO

Keywords:
Lava tunnel
Tumulus
Inflation
Stratovolcano
3D digitization
Effusion

ABSTRACT

Somma-Vesuvius is well known for its powerful Plinian explosive eruptions, however during the last eruptive cycle (1631–1944), persistent activity took place on the stratovolcano as mild and violent Strombolian, and effusive eruptions, forming more than one hundred lava flow fields. An important mechanism of lava transport within lava flow fields is the formation and development of lava tubes. The presence of lava tubes in a flow field can greatly increase their distance of emplacement. Observations of lava tubes at Vesuvius have been documented in historical records and speleological reports but no modern scientific studies are available. This work focuses on lava tubes formed in the compound lava flow field of the long-lived 1858 eruption (from 27 May 1858 to 12 April 1861) that was fed by seven eruptive fissures. The temporal and spatial evolution of the 1858 lava flow field was reconstructed using historical documentation. The exposed lava flow field surface was analysed using a 1-m resolution lidar Digital Surface Model (DSM). Surveys to fully digitize the interior and the overlying surface of the largest lava tube found in the 1858 lava flow field were conducted using a terrestrial laser scanner, optical cameras, and an Unmanned Aerial Vehicle (UAV). The accurate 3D model obtained was used to precisely quantify the inner dimensions and to better constrain the morphologies of the lava tube. Observed internal features were described and used to gain information on the formation and activity of the lava tube. Our data allowed us to understand that the described lava tube formed as an inflated lava flow inside which lava flowed through during an extended period ultimately draining out completely at the end of the eruption. Understanding how lava flow fields develop and how lava tubes form on Vesuvius is crucial to re-evaluate the last effusive activity of the volcano and its impact on hazard assessment.

1. Introduction

Somma-Vesuvius is one of the first and most studied volcanoes in the world. Most of the attention of the scientific community was on its explosive activity, especially on the famous 79 CE Plinian eruption. However, the last eruptive cycle of Vesuvius, that started in 1631 with a sub-Plinian eruption and stopped in 1944, was predominantly effusive (Carta et al., 1981; Arno et al., 1987; Arrighi et al., 2001; Cioni et al., 2008; Santacroce et al., 2008). For this eruptive activity many historical descriptions, chronicles of the time, drawings, paintings, and maps are available. Modern studies on the effusive activity of Vesuvius are limited in comparison to the ones on its explosive behaviour. Apart from the works of Belkin et al. (1993), Trigila and De Benedetti (1993) and Villemant et al. (1993) on the petrology and mineralogy of the lavas of Vesuvius and the study of Ventura and Vilardo (2008) on the 1944 lava flows, the emplacement mechanisms of lava flows on Vesuvius and their associated surface features were not fully investigated. During more than three hundred years, over one hundred lava flows were emplaced on the slopes of Vesuvius. Despite the low hazard linked to effusive eruptions due to the usually slow progression of lava flows, they can still

* Corresponding author.
E-mail address: thomas.lemaire@unina.it (T. Lemaire).

https://doi.org/10.1016/j.jvolgeores.2024.108197
Received 2 May 2024; Received in revised form 10 September 2024; Accepted 27 September 2024
Available online 29 September 2024

pose a danger for populations living on the flanks of volcanoes (Duncan et al., 1996; Chester et al., 2007). In the past, fatalities caused by lava flows have occurred (Harris, 2015; Brown et al., 2017). The main problem caused by lava flows for the population is the destruction of immovable properties like houses, businesses, agricultural lands, and critical facilities such as schools, hospitals, roads, and administrative buildings (Coltelli et al., 2012; Jenkins et al., 2017; Del Negro et al., 2019; Carracedo et al., 2022; Meredith et al., 2022, 2024). Lava flows can also cause secondary hazards such as wildfires or air pollution (Ainsworth and Boone Kauffman, 2009; Vasconez et al., 2018; Filippi et al., 2021; Carracedo et al., 2022; Hernández et al., 2022).

An important mechanism of lava transport in lava flows is by the development of lava tubes (Swanson, 1973; Greeley, 1987). Lava tubes are defined as 'roofed conduit of flowing lava, either active, drained or plugged' (Kauahikaua et al., 1998; Halliday, 2003), and in this study we apply this term independently of their shape or size. The presence of lava tubes can significantly increase lava flow length due to the insulation of the hot molten lava by an overlying cooled crust (Swanson, 1973; Peterson et al., 1994; Keszthelyi, 1995; Witter and Harris, 2007). Lava tubes on basaltic volcanoes are thoroughly described and their formation has been observed in active flows (Greeley, 1971a, 1971b, 1987; Hon et al., 1994; Peterson et al., 1994; Calvari and Pinkerton, 1998; Kauahikaua et al., 1998) or theorized through the study of cooled lava tubes (Atkinson et al., 1975; Calvari and Pinkerton, 1999). Five formation mechanisms of lava tubes by channel roofing or inflation have been theorized: (1) the rooted crust mechanism; (2) the accretional levees mechanism; (3) the slabs aggregation mechanism; (4) the pahoehoe lobe extension mechanism; and (5) the inflation lava mechanism (Greeley, 1971a, 1971b, 1987; Hon et al., 1994; Peterson et al., 1994; Calvari and Pinkerton, 1998; Kauahikaua et al., 1998; Sauro et al., 2020).

The flanks of Vesuvius are intensely urbanized with more than 300,000 inhabitants (Pesaresi et al., 2008; Harris et al., 2016) presently living in the path of lava flows emplaced from 1669 to 1944. On Vesuvius, lava flows from the last eruptive cycle primarily affected the western and southern flanks, occasionally reaching the coastline, more than seven kilometres away from the summit cone. Urbanization around Vesuvius continues to expand, especially in municipalities along the coastline, which are currently the most densely populated (Petrosino et al., 2004). Several rural dwellings are located at the footslopes of Vesuvius, and many houses or residential complexes have been built around the half of last century along the main roads which from the towns of Ercolano and Torre del Greco reach the crater. Consequently, in the event of an effusive eruption, the risk of lava flow destroying buildings is very high. Although lava tubes are commonly observed in basaltic lava flows (Ollier and Brown, 1965; Greeley, 1987; Peterson et al., 1994; Kauahikaua et al., 1998), some have been observed in phonotephritic lava flows (Belkin et al., 1993) of Vesuvius (Palmieri, 1859; Phillips, 1869). Malladra (1917) describes a lava tube in the 1858 lava flow that emplaced on the western slopes of Vesuvius. This lava tube was visited in 2006 by speleologists (Damiano and Del Vecchio, 2006), but no scientific investigations were carried out either on the 1858 lava flow field of Vesuvius nor on its lava tubes.

In this study, we focus our interest on the 1858 lava flow field of Vesuvius as it was produced by a long duration eruption, shows a large variety of surface features, and is up-to-now the only flow field with preserved and accessible lava tubes at Vesuvius. We present a reconstruction of the temporal and spatial evolution of the 1858 lava flow field and an analysis of its surface features. We describe the morphology and internal features of the lava tubes found in this lava flow field and analyse in detail the morphology of the largest lava tube using high-end technology. Finally, based on all the observations, we propose an interpretation of the mechanism that allowed the formation and development of the largest lava tube.

2. Geological setting

2.1. Somma-Vesuvius

The Somma-Vesuvius complex is located in the southern part of Italy, to the East of Naples in the southernmost part of the Campanian plain (Fig. 1a). The Somma-Vesuvius is a composite stratovolcano formed by (a) a pre-existing edifice, Monte Somma, that has collapsed repeatedly in consequence of highly explosive eruptions to form a composite caldera (Cioni et al., 1999; Arrighi et al., 2001; Cioni et al., 2008), and (b) a younger cone, Vesuvius (1281 m a.s.l) that grew after the 79 CE Plinian eruption (Cella et al., 2007; Cioni et al., 2008). Four major Plinian eruptions were identified: Pomici di Base (22,000 yr BP), Mercato (8800 yr BP), Avellino (3800 yr BP) and Pompeii (79 CE) (Santacroce et al., 2008). The last eruptive cycle of Vesuvius started after the sub-Plinian eruption of 1631 and continued as a prolonged period of open conduit condition with mainly effusive eruptions intercalated by Strombolian and Hawaiian eruptions (Carta et al., 1981; Arrighi et al., 2001). Eighteen cycles of activity separated by short repose periods, maximum seven years long, were characterized by Arno et al. (1987). This eruptive cycle ended with the 1944 eruption that destroyed the village of San Sebastiano (Chester et al., 2007; Cubellis et al., 2016). Following this event the volcano entered in a phase of quiescence that continues to date. The lava flows emplaced during the 1631–1944 cycle have both 'a'ā and pāhoehoe surfaces. Lavas erupted on Vesuvius have in majority phonotephritic compositions, with few basanites and trachy-basalts (Belkin et al., 1993). Lavas show a range of silica content from 47.00 to 49.30 wt% with a mean of 48.00 wt% and a high alkali content ranging from 6.42 to 11.87 wt% with a mean of 9.60 wt% (Belkin et al.,

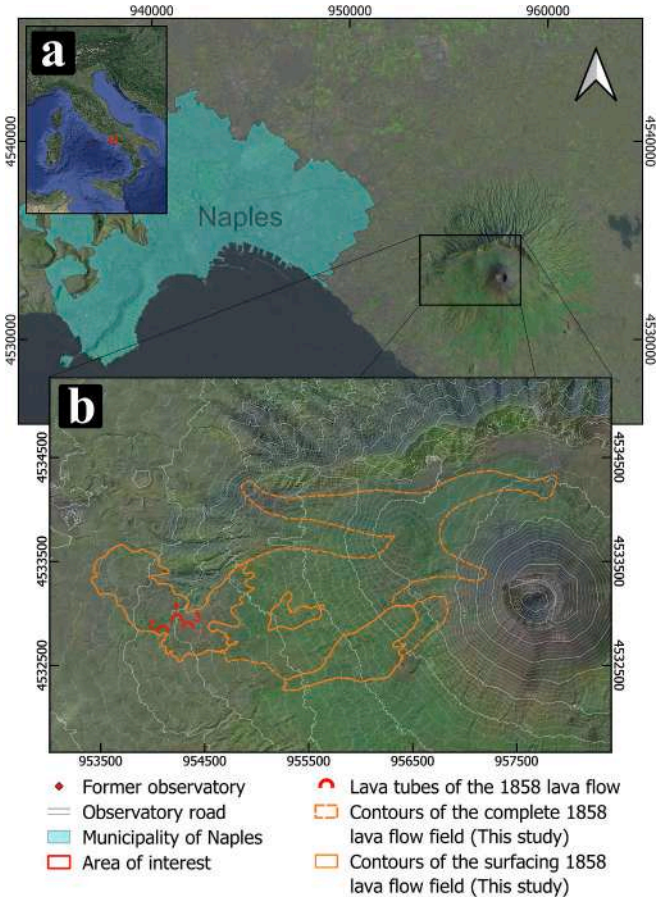

Fig. 1. a) Location of Vesuvius on the west coast of southern Italy, east of the city of Naples; b) Location of the 1858 lava flow and its lava tubes on the west flank of Vesuvius.

1993). Lavas are porphyritic with an average of 40 % phenocrysts mostly leucites and clinopyroxenes (Trigila and De Benedetti, 1993).

2.2. The 1858 eruption

Like many eruptive events on Vesuvius, the 1858 eruption was observed by the inhabitants of the Naples Bay but also by tourists and scientists coming from Western Europe. Several books were published on the volcanoes of Southern Italy (Hamilton, 1772; Mercalli, 1884; Johnston-Lavis et al., 1891) describing the eruptions of Etna (Gemmellaro, 1819; Maravigna, 1819; Gemmellaro, 1844), Stromboli (Mercalli, 1881, 1888), Vulcano (Mercalli, 1888, 1889) and Vesuvius (Pigonati, 1767; Guarini et al., 1855; Phillips, 1869). Geological maps depicting the extent of lava flows were made (Marsigli, 1832; Roth, 1857; Le Hon, 1866; "Monte Vesuvio," 1860s (unknown precise publication date)). Many paintings and drawings were produced by artists or scientists capturing eruptions at a certain time or shedding light on strange phenomenon such as lava tubes (Phillips, 1869). Luigi Palmieri, director of the Vesuvius Observatory at the time, described in detail the course of the 1858 eruption up to July 1859 in the annals of the Observatory (Palmieri, 1859) and resume the 1858 eruption in a report to the Accademia Pontaniana (Palmieri et al., 1862). The 1858 eruption started on the 27 of May and lasted nearly three years to end the 12 April 1861 (Palmieri et al., 1862; Scandone et al., 1993). During this eruption, seven eruptive fissures opened, and a compound lava flow field emplaced on the western flank of Vesuvius (Fig. 1b). The lava flow field reached a maximum of five kilometres from the vents and inundated two deep valleys. Two samples of the 1858 lavas were analysed using X-ray fluorescence (XRF) by Belkin et al. (1993). Lavas are phonotephritic with a mean SiO_2 content of 47.45 wt% and a mean alkali content of 9.90 wt% (Belkin et al., 1993). Lavas of the 1858 eruption are strongly porphyritic with an average crystal content of 40 % (Trigila and De Benedetti, 1993). The 1858 lava flow has a pāhoehoe surface with a variety of surface features. These inflated surface features form by local overpressures that cause crustal uplift creating a few meters high reliefs (Walker, 1991; Rossi and Gudmundsson, 1996; Duncan et al., 2004; Anderson et al., 2012). The lava tubes we describe in this study are found in the shallowest portions of the flow field. Other and previous lava tubes might have been covered by the 1858 last lavas or by more recent lava flows (1895–1899, 1944), thereby obscuring them from observation. Up to now, these lava tubes are unique features on Vesuvius because they are the only ones discovered, preserved and accessible.

3. Materials and methods

3.1. Historical and contemporary documents

Historical documents were used to reconstruct the temporal and spatial evolution of the 1858 eruption, the 1858 lava flow field contours and to obtain information about lava tubes. We carried out a thorough literature review and found eight geological and topographical maps from 1832 to 2016 (Marsigli, 1832; Roth, 1857; Le Hon, 1866; "Monte Vesuvio," 1860s (Unknow author, unknown precise publication date); Istituto Geografico Militare, 1908a, 1908b; Santacroce and Sbrana, 2003; Paolillo et al., 2016). The two maps from 1832 (Marsigli, 1832) and 1857 (Roth, 1857) show the topography or the lava flows prior to the 1858 lava flow. The two maps from the end of the 1860s (Le Hon, 1866; Unknow author "Monte Vesuvio," 1860s (unknown precise publication date)) show the 1858 lava flow before being largely covered by the 1895–99 lava flow. The four other maps were published in 1908 (Istituto Geografico Militare, 1908a), 1908 (Istituto Geografico Militare, 1908b), 2003 (Santacroce and Sbrana, 2003) and 2016 (Paolillo et al., 2016).

Moreover, we analysed paintings of the 1858 eruption (Fig. 2a, b) to better reconstruct its development through time. We also used a precise description of the evolution of the 1858 eruption by the director of the Vesuvius Observatory, Luigi Palmieri, reported in the 1859 Annals of the Vesuvius Observatory. In the literature, an important paper from Malladra was published in 1918 where the author described in detail the lava tube formed by the 1858 lava flow of Vesuvius.

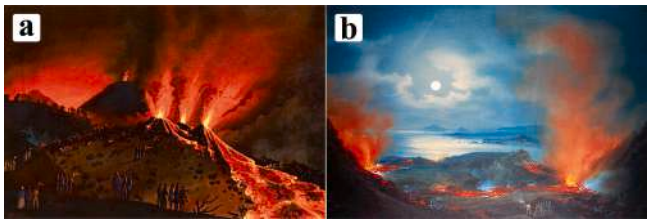

Fig. 2. Paintings of the 1858 eruption. a) painting with a point of view from the observatory by an unknown artist, private collection; b) Painting Chiaro di Luna durante l'eruzione del 1858 by Giovan Di Battista Gatti representing the 1858 eruption during a full moon, 48 h after its beginning, from the north side of the Gran cono.

3.2. Topography

Two different elevation datasets were used to describe lava flow morphology, lava flow surface and lava tubes surfaces: a Digital Terrain Model (DTM) with a 1-m resolution from the municipality of Naples (www.cittametropolitana.na.it/pianificazione_territoriale/) and a DTM covering the entire Italian territory with a 10-m resolution from the Tinitaly project (Tarquini et al., 2023) of the Istituto Nazionale di Geofisica e Vulcanologia (INGV). From the 1-m DTM we extracted three topographic parameters: slope, relative relief, and aspect (Ventura and Vilardo, 2008). Slope and aspect were calculated using the Horn formulas (Horn, 1981). Relative relief was calculated as the difference between minimum and maximum altitude within a five pixels radius to highlight fine scale features and within a hundred pixels radius to identify large scale features. We produced precise Digital Elevation Models (DEM) of the overlying surface of the lava tube in order to describe precisely the morphology of the surface over the lava tube. The proceedings to scan this surface are described in the next section.

3.3. 3D scanning of the lava tube

The lava tube interior was captured using a time-of-flight terrestrial laser scanner (TLS), the Riegl VZ-400, which has an angular measurement resolution of 0.0005° (Fig. 3a). The data was acquired during field work in March 2024. Nineteen scans from different points of view were necessary to obtain a satisfactory result by minimizing shadow areas produced by the morphology of the tube (collapses, tube extensions). Reflectors of varied sizes were used for common points of reference between the scans. Twelve out of the nineteen scans made during the survey (Fig. 3b) were used to build the 3D model in RiSCAN Pro. Additionally, photogrammetry work was performed in the northern and southeastern points of the tube using a Gopro 10 camera to complete the 3D scan obtained by the TLS.

The overlying surface of the lava tube was scanned using a DJI Matrice 300 RTK UAV. Markers were placed on and in the lava tube to facilitate scan alignment. Three flights were performed in March 2024. (1) A global photogrammetric survey of a large area around the lava tube was carried out using the UAV equipped with a Zenmuse P1 optical camera. (2) A low altitude flight over the lava tube using the same optical camera, and (3) a survey using the UAV equipped with a Zenmuse L1 LiDAR (Light Detection And Ranging) sensor were done. The optical data was processed in Agisoft Metashape Professional to obtain point clouds, meshes and DEMs, while the LiDAR data was treated using the DJI Terra software.

Another survey of key parts of the lava tube, the skylight and a large fracture in the roof, was conducted with a Gopro 10 camera to perform

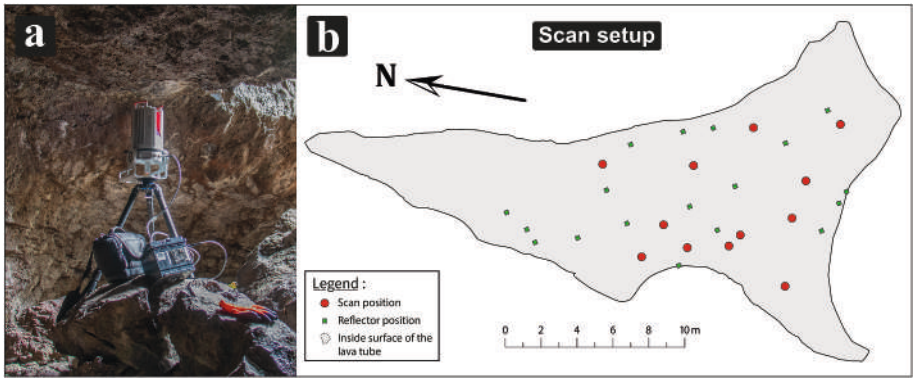

Fig. 3. 3D scan setting. a) Photograph of the Riegl VZ-400 terrestrial laser scanner during the lava tube survey; b) Scan and reflector positions into the lava tube.

photogrammetry work. This survey allows the connection between the scanned georeferenced surface and the scanned interior. These images were transformed into point clouds and meshes with textures using Agisoft Metashape. The 3D scan of the interior of the lava tube was aligned with the georeferenced DTM surface in CloudCompare to form a complete 3D representation.

4. Results

4.1. The 1858 lava flow field

4.1.1. The 1858 eruption and the emplacement of the lava flows

The historical documents that describe the 1858 eruption were used to reconstruct its temporal and spatial evolution (Fig. 4). The complete contour of the 1858 lava flow field and the position of the vents were extrapolated from old geological maps (Le Hon, 1866; Unknow author, "Monte Vesuvio," 1860s (unknown precise publication date); Istituto Geografico Militare, 1908a, 1908b; Santacroce and Sbrana, 2003; Paolillo et al., 2016). From the descriptions of the 1858 eruption, we extracted the position and formation time of the different vents, but also the position and direction of the flow fronts and the size and speed of the lava flows at different dates.

In the 1859 Annals of the Vesuvius Observatory, Palmieri described the 1858 eruption (See Table 1) by saying that it started with the opening of a fissure in the west side of the Gran Cono (the cone that grew within the Monte Somma caldera, now called Vesuvius) on the 27 of

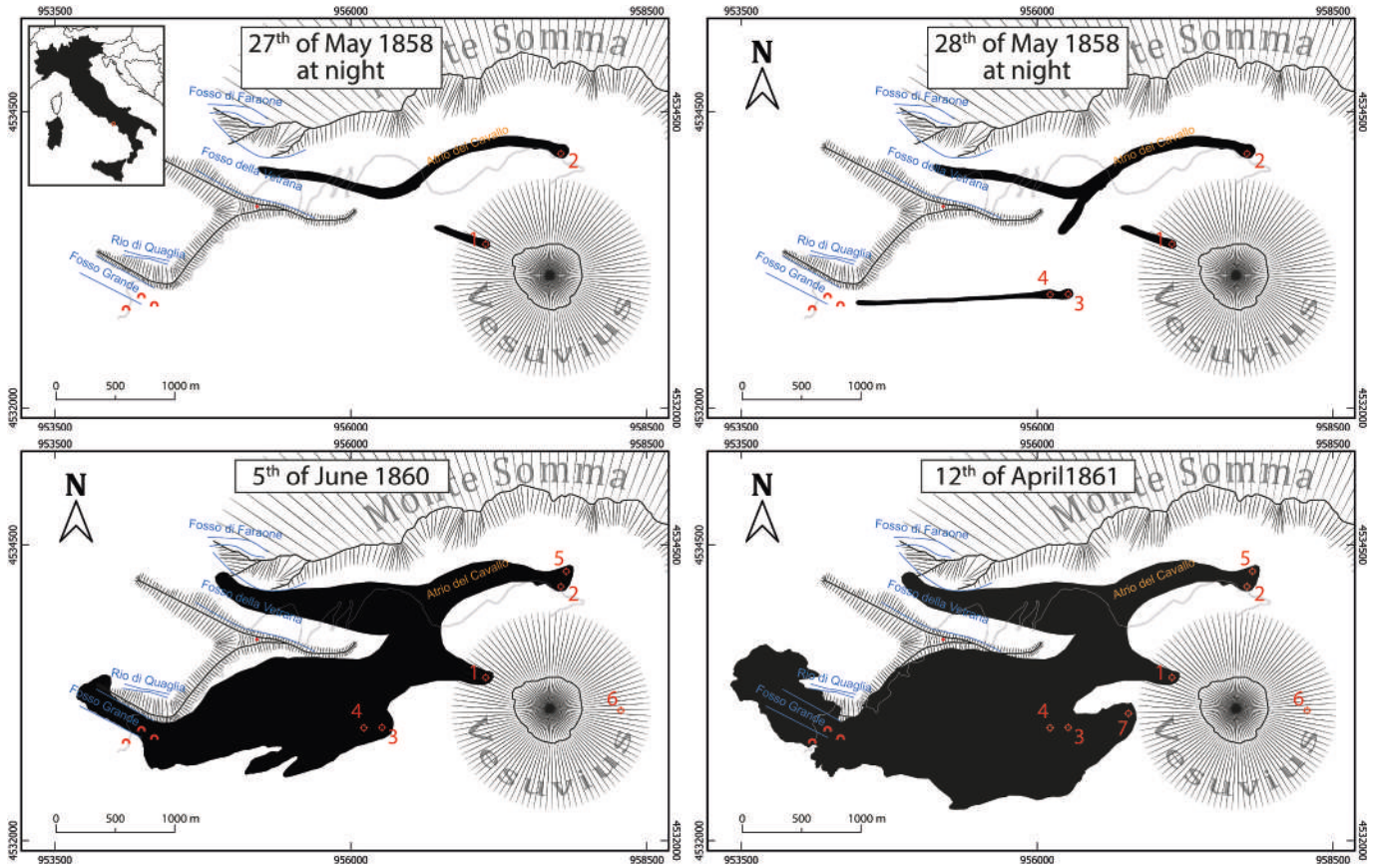

Fig. 4. Sketches of the temporal and spatial evolution of the 1858 lava flow field reconstructed using historical documents, paintings and geological maps. Fissures or vents are red circles. Lava flow is solid black. Blue lines are the boundaries of the main actual and past valleys. Red diamond is the position of the former Observatory. (For interpretation of the references to colour in this figure legend, the reader is referred to the web version of this article.)

Table 1
Chronology of events for the 1858 eruption of Vesuvius.

Date	Time	Event
27 May 1858	4:17 a.m.	Opening of vent 1 on the western side of Vesuvius.
27 May 1858	Not mentioned	Opening of vent 2 in the Atrio del Cavallo.
28 May 1858	4:30 a.m.	Opening of vent 3 in the Piano delle Ginestre.
28 May 1858	Not mentioned	Opening of vent 4 next to fissure 3. Opening of vent 5 next to vent 2. Opening of vent 6 on the eastern side of Vesuvius.
Not mentioned	Not mentioned	Closure of vent 6 after low emission of lava.
15 June 1858	Not mentioned	Closure of vent 1,2 and 3. The eruption seemed to have come to an end but vent 4 and 5 still emit.
30 June 1858	Not mentioned	Closure of vent 5 after a month of activity.
March 1860	Not mentioned	Closure of vent 4 after nearly two years of activity, eight days later, opening of vent 7.
12 April 1861	Not mentioned	Closure of vent 7 after a year of activity, end of the eruption after 1051 days of activity.

May 1858 at 04:17 a.m. He observed the opening of a second fissure on the same day (precise time of opening is not mentioned by Palmieri) in the Atrio del Cavallo and at the end of the 27 of May, he saw that the lava erupting from this vent was starting to flow into the Fosso della Vetrana (Fig. 4). Palmieri calculated that, on the 27 of May, the lava had a velocity of 2 ms^{-1}. The next day, he stated that a third fissure opened in the Piano delle Ginestre at 04:30 a.m. (Fig. 4). Soon he observed a fourth vent opening next to the third and abundant lava flowing out of it (precise time of opening is not mentioned by Palmieri). This painting by Giovan Battista Gatti called "Chiaro di luna durante l'eruzione del 1858" represents the 1858 eruption during a full Moon seen from the north side of the Gran Cono (Fig. 2b). We determined the date on which the artist painted this representation using a mean lunar cycle of 29 days, 12 h, 44 min, and 3 s (29.53058885 days). The painting was probably depicted during the night of Friday 28 of May 1858, about 48 h after the beginning of the eruption. The overall extension of the flows at that time can be determined using this painting. Palmieri described the development of the eruption noting that the lava was then flowing into a ~ 100-m-deep valley called Fosso Grande. He described the opening of a fifth fissure next to the second one and the opening of a sixth fissure in the eastern part of the Gran Cono from which a moderate amount of lava flowed out.

According to Palmieri, most of the vents stopped emitting lava after a few days to a few weeks. He noticed that vents 4 and 5 were the only ones active on the 16 of June 1858 and that fissure five stopped emitting on the 30 of June 1858. Palmieri wrote in a report to the Accademia Pontaniana that only fissure 4 in the Piano delle Ginestre kept emitting lava until the end of March 1860 (Palmieri et al., 1862). Eight days after the closure of vent 4, a seventh fissure opened 600 m higher and emitted lava until the 12 of April 1861 (Palmieri et al., 1862; Scandone et al., 1993).

4.1.2. Flow margins of the 1858 lava flow

Six historical and recent geological maps from the 1860s to 2016 were used to extrapolate the flow margins of the 1858 lava flow field. When georeferenced into a GIS (Fig. 5), discrepancies between the covered areas appear. Some discrepancies are related to the deposition of new lava flows after 1858, some are dependent on the choices of the authors, and some are due to errors during the georeferencing of the oldest geological maps. In an attempt to overcome the addressed discrepancies amongst geological maps, new margins were redefined, one of which represents the outline of the exposed 1858 lava flow field and the other represents the outline of the complete lava flow field. Both were defined based on the geological maps, on the 1-m and 10-m resolution DEMs and on detailed field work (Fig. 5). Using these new flow margins, we measured that the area of the complete flow field is 3.9 million square meters and that the exposed area is 1.3 million square meters which implies that 66 % of the 1858 lava flow field is covered by other flows. Centre lines were determined using the methodology of Kereszturi et al. (2016). A minimum flow field length of 3.069 km and a maximum of 5.207 km were measured. We measured the width of the lava flow field every hundred meters along the centre lines, the mean width being 0.607 km with a minimum width of 0.116 km and a maximum width of 1.496 km. Volume and thickness of the 1858 lava flow field are not measurable but will be estimated in the following sections.

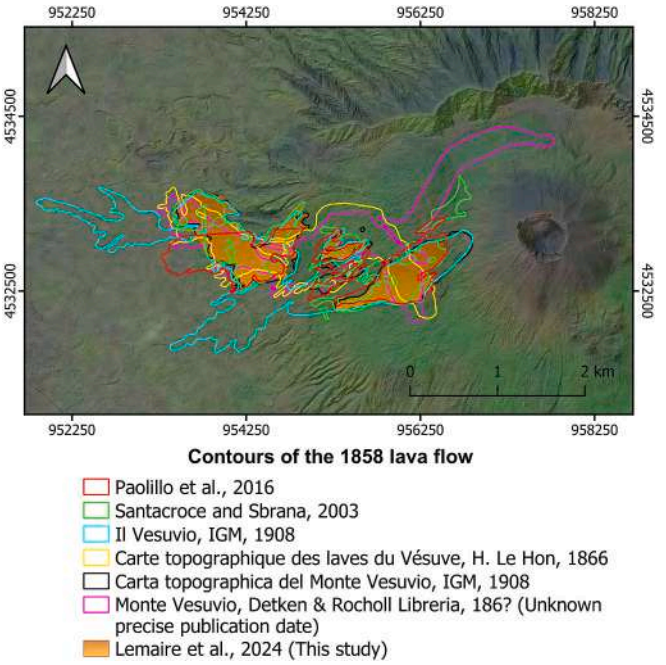

Fig. 5. Representation of the flow margins of the 1858 lava flow field extracted from six georeferenced historical and recent geological maps (coloured lines) and from the results of this study (solid orange).

4.1.3. Topographic parameters and surface features

Using the 1-m DEM of Vesuvius, a surface analysis of the 1858 lava flow field was carried out. Three topographic parameters were used to describe the still exposed part of the 1858 lava flow field (Fig. 6): slope, relative relief, and aspect (Ventura and Vilardo, 2008). The slope of the surface is comprised between 0.01° and 84.41° with an average of 15.87°. Three breaks in slope are visible in the western part of the lava flow field. The relative relief calculated using a five meters radius shows a large number of very fine-scale features with a mean difference of altitude of 0.17 m. These correspond to small tumuli or tilted slabs of lava. On the other hand, the relative relief calculated using a one hundred meters radius shows tens of large-scale features. These correspond to large tumuli a few meters high or dome-shaped features up to sixty meters in diameter. These large surface features are mostly present in the western distal part of the lava flow field, while the eastern proximal part has a flatter surface (Fig. 6). Similarly, the aspect shows these large-scale features but also the overall south to north south direction of the lava flow. We can observe more surface features in the distal part of the lava flow field, but the description of the lava flow field surface is made

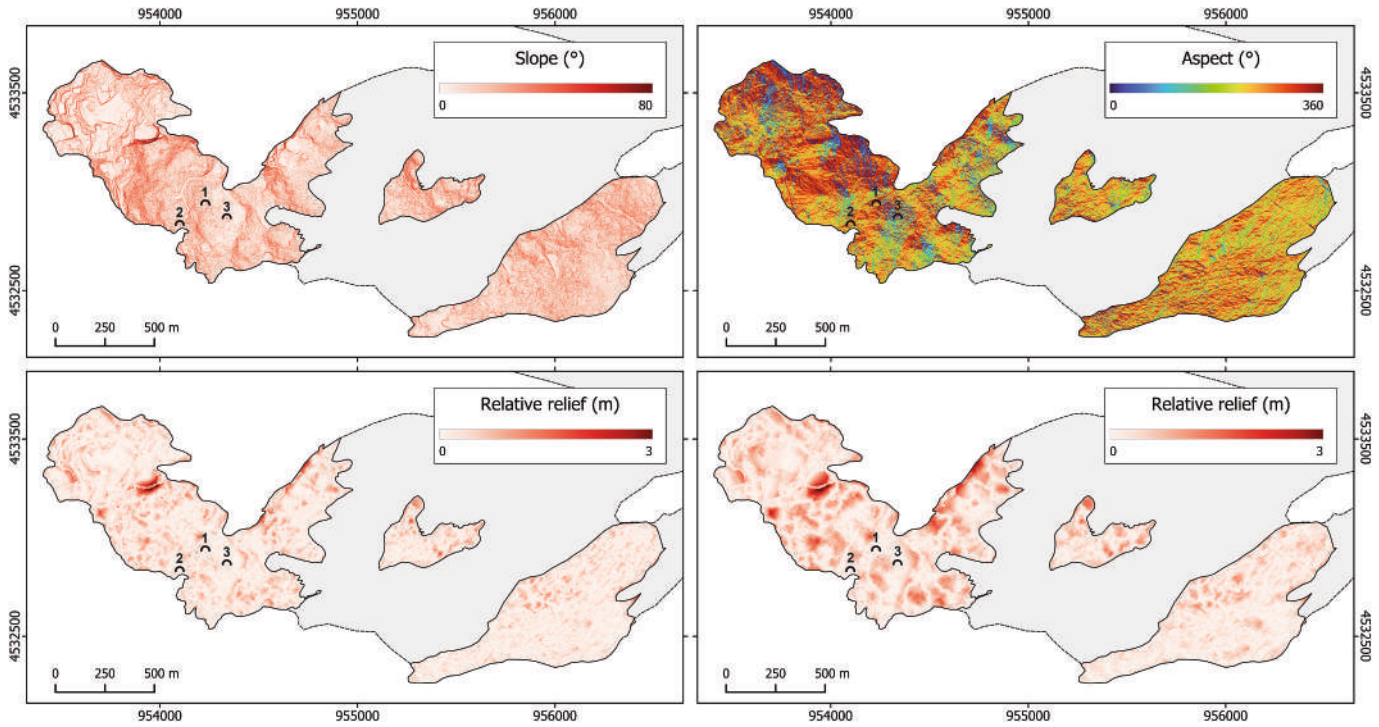

Fig. 6. Surface parameters for the exposed areas (uncovered by more recent lava flows) of the 1858 lava flow field. Top left, slope. Top right, aspect. Down left, relative relief with a radius of 5 m. Down right, relative relief with a radius of 100 m.

difficult by covering of more recent lava flows and by the presence of dense vegetation.

4.1.4. *Estimation of the emitted volume and eruption rates*

Using the historical description of the 1858 eruption (Palmieri, 1859), we know the opening and closing times of the eruptive vents (Fig. 7). Vents 1 and 2 opened the first day followed by vents 3 and 4 the second day and by vents 5 and 6 the fourth day. Most of the vents stopped emitting lava after a few days to a few weeks. Vents 1, 2 and 3 stopped erupting on the 15 of June 1858, twenty days after the beginning of the eruption. Vent 5 stopped emitting lava on the 30 of June 1858, after thirty-two days of activity. The closing of vent 6 was not described but probably occurred a few days after its opening as Palmieri wrote that a moderate amount of lava was emitted from this vent. Only

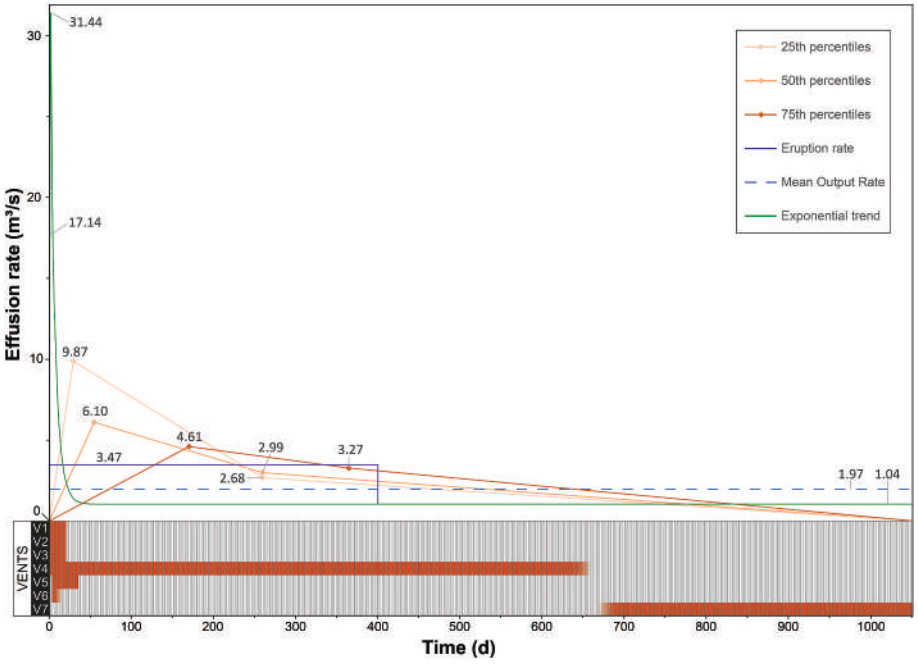

Fig. 7. Opening and closing time of the eruptive vents of the 1858 eruption and estimated eruption rates. Eruption rate estimated based on the volumes of Palmieri (solid blue line), mean output rate of the 1858 eruption (dashed blue line), characteristic effusion rates for the 1858 eruption based on the characteristic curves from Zuccarello et al., 2022 (solid orange lines) and exponential effusion rate trend based on the estimated volume and mean output rate of the 1858 eruption (solid green line). (For interpretation of the references to colour in this figure legend, the reader is referred to the web version of this article.)

vent 4 kept emitting lava until March 1860. Vent 7 opened eight days after the closure of vent 4 and was the only vent to emit until the end of the eruption.

Palmieri estimated an erupted volume of 120 million cubic meters of lava in July 1859, with 36 million cubic meters emitted from vent 4. This value is inevitably underestimated because the eruption stopped more than eight months later. If we consider the time of emission of this volume from the 27 of May 1858 to the 1 of July 1859 (400 days) and use the eruption rate equation:

$$Q = Vt/t \quad (1)$$

then the mean eruption rate during this period is 3.47 m^3s^{-1} (Fig. 7). We calculated the eruption rate at vent 4 which is 1.04 m^3s^{-1} for the same period. Using the average eruption rate of the whole flow field from day 1 to day 400 and the eruption rate of vent 4 for the rest of the eruption, we estimated the total volume of the lava flow field at the end of the eruption (after 1051 days of eruption) to be 178 million cubic meters. The mean 1858 flow field thickness is then equal to 45.85 m. The thickness of the flow field can seem high compared to other flows at Vesuvius like the 1944 lava flow that has a mean thickness between 6 and 17 m (Ventura and Vilardo, 2008). This difference could be explained by the pre-emplacement topography, consisting in deep valleys cut within pyroclastic deposits, by the compound morphology of the flow field and by the long duration of the eruption. Based on the calculated volume and duration of the eruption we estimate the mean output rate to be 1.97 m^3s^{-1}.

To have an idea of the emplacement dynamics, it is necessary to define effusion rate trends, namely both the trends based on eruption duration and a trend based on initial effusion rates, estimated volume and mean output rate. We used the characteristic effusion rate curves identified on Etna by Zuccarello et al., 2022; Fig. 7) as for lava flow morphology, erupted volumes, and emplacement on steep slopes, eruptions at Etna are similar to those that occurred during the 1631–1944 cycle of Vesuvius, thus making the work of Zuccarello et al. (2022) a good proxy to estimate eruption rates. There are three curves corresponding to the 25th, 50th and 75th percentiles of the occurrence of effusion peaks. These curves have classic waxing and waning phases. Applied to the 1858 eruption, these characteristic curves yield instantaneous effusion rates attaining maximum effusion peaks of 4.6 to 9.9 m^3s^{-1} after 29 to 170 days of eruption and diminishing to 2.7 and 3.3 m^3s^{-1} (respectively) after 260 to 365 days.

We defined an exponential curve to represent a waning phase after

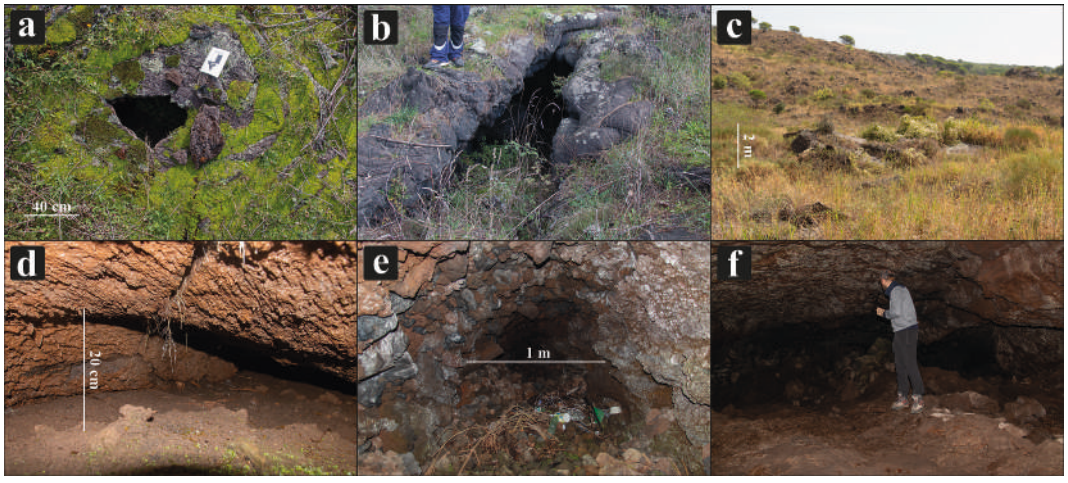

Fig. 8. Photographs of the three lava tubes found in the 1858 lava flow field. a) Exterior surface of tube 1; b) Exterior of tube 2; c) Exterior surface of tube 3; d) Interior of tube 1; e) Interior of tube 2; f) Interior of tube 3.

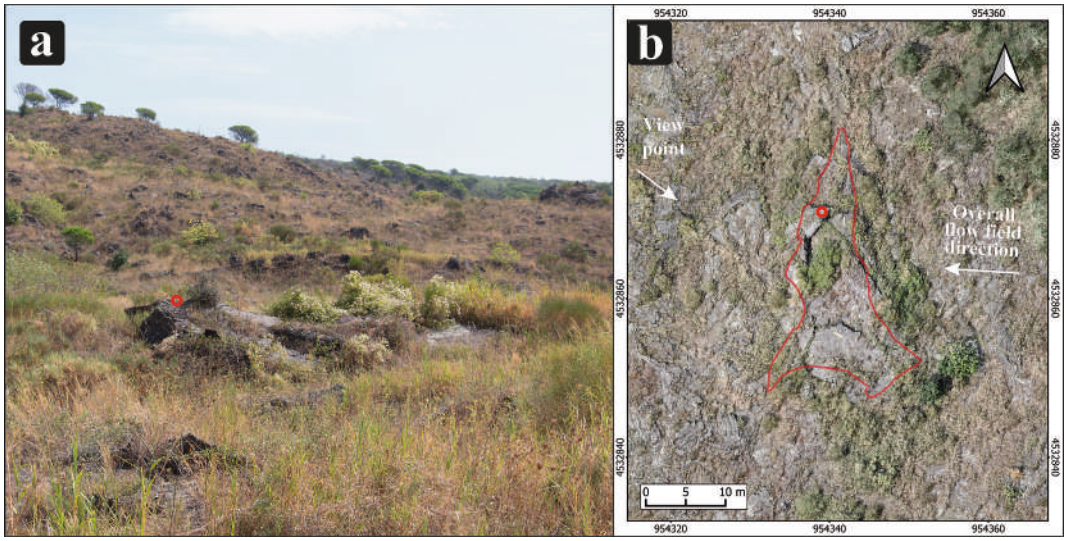

Fig. 9. Lava tube surface. a) Photograph of the lava tube surface from the north west with a reference point (red circle); b) colorized DEM with the contour of the lava tube (solid red line) and a reference point (red circle). (For interpretation of the references to colour in this figure legend, the reader is referred to the web version of this article.)

the effusion peak using the equation from Wadge, 1981; Fig. 7):

$$Q_t = Q_0 e^{-\lambda t} \quad (1)$$

In which Q_0 is the initial effusion rate and λ a constant. Firstly, we calculated the effusion rate at each vent after 15.5 and 39.5 h from the beginning of the eruption using the equation of Wadge (1978) that is based on the length of the lava flow:

$$Q = 4.8L \quad (2)$$

This equation yields a total effusion rate of 17.14 $m^3 s^{-1}$ at 15.5 h and 31.44 $m^3 s^{-1}$ at 39.5 h. We modified eq. (1) as:

$$Q_t = Q_p e^{-\lambda t} + c \quad (3)$$

Where Q_p is the effusion rate at its peak, and c a constant. Constrained by the volume of the lava flow field and the mean output rate of the eruption, eq. 3 becomes:

$$Q_t = 31.44 e^{-(0.154t)} + 1.04 \quad (4)$$

4.2. Lava tubes in the 1858 lava flow field

4.2.1. Description of the lava tubes

We found three lava tubes in the distal part of the 1858 lava flow field (Fig. 1b), each showing a different size and morphology. The first one is a small lava tube, labelled 1 in Fig. 1, located next to a tumulus, and formed in one of its pahoehoe lava outpourings (Fig. 8a). Its roof is formed by two thin layers of ropy pāhoehoe lava and is a few centimetres thick. This small lava tube has a twenty centimetres internal diameter (Fig. 8d). The second, labelled 2 in Fig. 1, is located in a steep part of the 1858 lava flow field. It is an early-stage lava tube that was probably active for a few hours to a few days. It is five meters long and nearly two meters high (Fig. 8b). Inside we observed 'a'ā rubbles fringed by squeezed out toothpaste pāhoehoe (Fig. 8e). The third one, labelled 3 in Fig. 1 (Fig. 8c, f), is the largest found in the 1858 lava flow field and possibly the largest ever found at Vesuvius. It is located in a very flat area of the flow field. Its morphology is described in detail in the next section.

4.2.2. Morphology of the largest lava tube

On the different Digital Elevation Models showing the 1858 lava flow field, the largest lava tube appears as a triangularly shaped relief one to two meters high oriented north south (Fig. 9). A skylight, by which it is possible to enter the lava tube, appears as a small depression. The high-resolution DEM of the lava tube surface produced by UAV photogrammetry shows the slabs of ropy pāhoehoe lava forming the roof of the lava tube and the fractures separating them. The exterior of the lava tube has a strong morphological resemblance to a tumulus.

Inside, the lava tube (Fig. 10) also has a triangular shape with a length of 30.15 m (A-R) in the north south direction and a width that varies from 1.20 m at the northern point (A) to a maximum of 17.41 m in its southern part (S-B). We measured a mean inside height of 1.40 m with a maximum height of 2.47 m in the southern part of the lava tube (Fig. 10). Flow direction in the lava tube was from north to south. The lava entered by a twenty-five centimetres wide vent and exited the lava tube to the southwest by a small passage at point C (Fig. 10). A section of 34.46 m along that flow path (A-M-C) showed an average slope of 4.43°. The slope inside the tube from B to S is 2.80°. We defined a plane by taking three points at the tips of the tube (A, B and C) and calculated an overall slope of 5.05° to the southwest. We measured the internal floor surface of the lava tube being 222.6 m^2 and the actual volume of the lava tube being 328 m^3 ± 41 m^3. An area of the roof collapsed forming a skylight, from where it is possible to enter the lava tube. In addition, several blocks fell from the roof covering some sections of the floor of the lava tube. This is especially true under the east west fracture at point M (Fig. 10) where a large pile of rock debris is present. For every vertical section, we measured the roof thickness at distances of one meter. The mean roof thickness is 2.40 m for the A-C section, 2.15 m for the A-R section, 2.73 m for the S-B section and 2.19 for the *E*-T section (Fig. 10). The overall roof thickness is 2.37 m with a thinner area of 0.74 m and a thicker area of 4.29 m.

Taking into account the resources available at the time, Malladra masterfully described the overall morphology of the lava tube in comparison with our high-resolution model (Fig. 11). However, few differences appear when we compare the same sections as Malladra drew and using the same points of reference. One of the main differences is at the southern end of the lava tube where the eastern extension is narrower in the drawing of Malladra. On his sections, he measured 33 m for the A-R distance, which is 3 m longer than our measurement. Malladra measured 42.80 m for the flow path A-M-C, which is more than 8 m longer than what we measured. B-C length is 24 m on his drawings, more than 6 m longer than the length we measured. Malladra measured a difference of altitude between point A and point C of 3 m, corresponding to a slope of 4.01°, which is very close to the 4.43° that we measured on the 3D model. These differences show the importance of new morphology

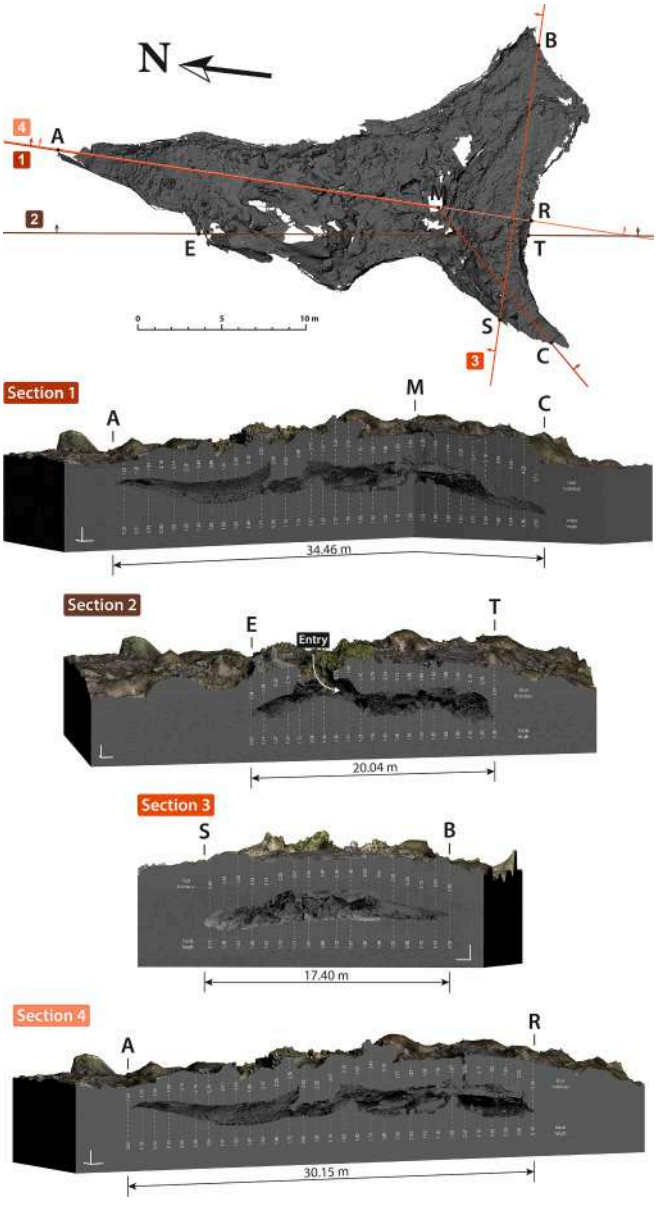

Fig. 10. Four axonometric 3D sections and cross-sections of the lava tube with measured roof thickness and inside height values every meter.

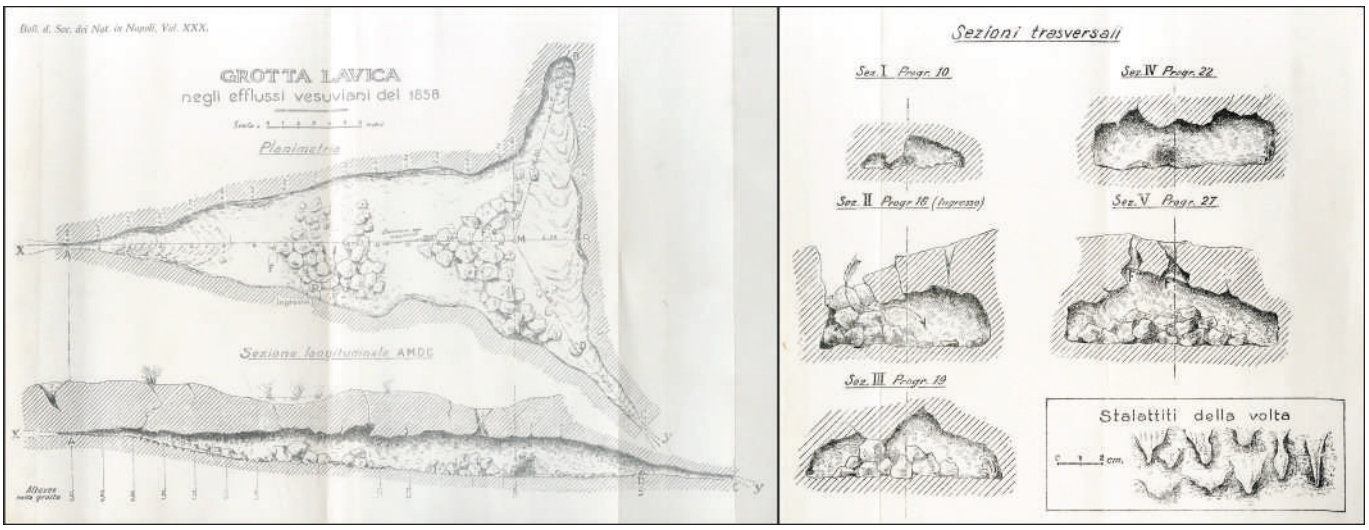

Fig. 11. Sections and cross-sections of the lava tube from Malladra (1917).

analyses using high-end technologies in order to obtain extremely detailed measurements.

4.2.3. *Internal features*

Inside the lava tube we observed several features showing evidence of prolonged lava flowage (Fig. 12). Where parts of the wall collapsed, we observed that the lava tube is lined with at least twelve, millimetres to centimetres thick, layers of lava (Fig. 12a). The thickness of those linings depends partly on the rheology of the lava that filled the tube, and the number of linings depends on the number of times the lava tube filled and drained (Calvari and Pinkerton, 1999). The last lining is five to seven centimetres thick indicating that a higher viscosity lava flowed into the lava tube before it ultimately emptied completely. In certain areas, this wall lining detached from the wall and rolled down on itself forming rolls on the sides of the lava tube (Fig. 12b). It indicates that the lava tube emptied rapidly while this lining was still plastic, in contrast with the outer linings that were already rigid and stable. In other areas, we can observe vertical grooves in the wall lining (Fig. 12c). This indicates a vertical drop of solid lava that marked the plastic wall lining when the flow suddenly dropped inside the lava tube flowing at a lower level. Gas blisters are visible on the walls of the lava tube where the last lining detached or collapsed (Fig. 12d, e). Their diameters are comprised between 4 and 10 cm. Gas blisters are remnants of gas bubbles that were present in between linings. Some of them indicate that the gas bubble was still surrounded by molten lava when the lining detached leaving thin glassy lava. The ceiling of the lava tube has large bulbous in shape features on its surface (Fig. 12f). On the roof at the northern and southwestern points of the tube (A and C, Fig. 10), small stalactites with a maximum length of two centimetres are present (Fig. 12g). These stalactites have smooth surfaces and are covered by a thin light brown glassy film. They have a cone-like shape and form along small ridges aligned in the flow direction. This type of stalactite is believed to be formed by remelting of the lava by hot gases accumulating at the roof of the tube (Peterson et al., 1994; Kauahikaua et al., 1998). On the walls of the lava tube, we also observed pull-apart stalactites where the lining detached. Those stalactites form by the stretching of still plastic lava in between two linings that confers them a spiky morphology (Calvari and Pinkerton, 1999). Their length is less than half a centimetre. Another type of stalactite can be observed on the walls of the lava tube as thin horizontal tubular features with a length up to half a centimetre (Fig. 12h). From a conical base, a thin tube goes out and at the tip of this kind of stalactite is usually present a small spherical piece of lava. Where a part of the wall collapsed, we can observe the coating of a portion of a block with fluid lava (Fig. 12i). The fissure that detached this block was

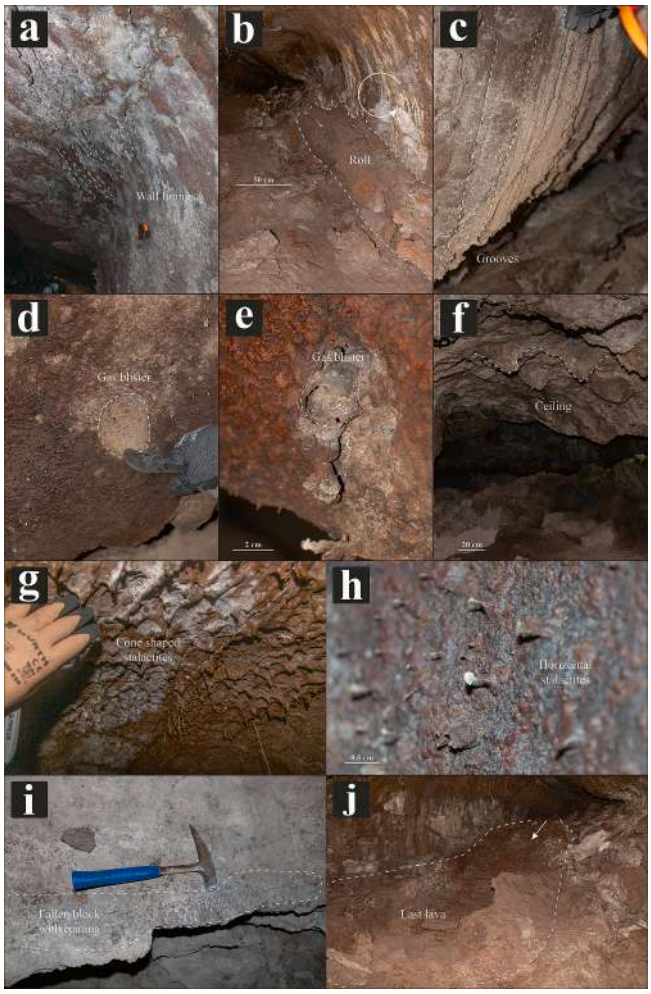

Fig. 12. Photographs of the observed internal features. a) Wall linings; b) Rolled down wall lining; c) Vertical grooves; d) Imprint of a gas blister; e) Gas blister; f) Bulbous in shape features on the lava tube ceiling; g) Cone shaped stalactites; h) Horizontal tubular stalactites; i) Lava coating on a fallen block; j) Last lava entering the lava tube.

formed before the lava tube emptied. The last lava that entered the lava tube via the entry point (Point A), flowed and solidified as a ropy pāhoehoe flow (Fig. 12j). It emplaced 6.60 m inside the lava tube and has a maximum width of 1.40 m. It is confined by 0.20 m wide levees.

5. Discussion

This study gives insights into lava flow emplacement and morphologies of lava tubes on Vesuvius. We conducted a spatial and temporal reconstruction of the 1858 lava flow field emplacement on Vesuvius, a detailed morphological and surficial analysis of the 1858 lava flow field and a complete morphological analysis of its associated lava tubes.

The 1858 eruption was a fountaining event with seven eruptive vents that formed a compound lava flow field that inundated deep valleys on the western flank of Vesuvius. The low eruptive rates and long duration of the 1858 eruption, as well as the confined emplacement topography contributed to the compound morphology of the lava flow field (Anderson et al., 2005). Most of the 1858 lava flow field shows a pāhoehoe surface with features that are evidences of inflation within the last flow-unit where the molten lava uplifted its overlying crust. These inflation structures are tumuli that inform us about local overpressures and flow accumulations that happened during lava flow emplacement. The western part of the 1858 lava flow, furthest from the vents, was much more affected by these processes.

After one hundred years, we reconsidered the presence of lava tubes in the 1858 lava flow field of Vesuvius and scientifically studied one of them using modern technologies. The 1858 lava flow has a phonotephritic composition, demonstrating the possibility of lava tube formation and development in volcanic systems that erupt more alkaline and highly porphyritic lavas such as Vesuvius.

We presented a detailed morphological analysis of the largest lava tube and its overlying surface using a complete 3D model of the area. In term of shape and size, the studied lava tube is much smaller and has a different morphology than lava tubes in basaltic settings such as Hawaii, Canary Islands, Iceland or Etna where lava tubes are hundreds to thousands of meters long, tens of meters wide, and shaped like meandrous rivers (Ollier and Brown, 1965; Greeley, 1971a, 1971b; Hróarsson and Jónsson, 1991; Peterson et al., 1994; Kauahikaua et al., 1998; Calvari and Pinkerton, 1999; Tomasi et al., 2022; Calvari et al., 2024). On Vesuvius, this lava tube is relatively small in size, measuring only 30 m in length, and has a triangular shape typical of a pāhoehoe breakout. A more reasonable comparison can be made with lava tubes formed at Mount Etna. One lava tube formed by pāhoehoe lavas at Mt. Etna is the 105 m long Mt. Arcimis lava tube (Calvari et al., 2024). While being small in size like the studied tube at Vesuvius, the Mt. Arcimis lava tube has a near tubular braided morphology. The morphology of the lava tube at Vesuvius shows signs of lava inflation processes, not as the succession and connection of pāhoehoe lobes (Crown and Baloga, 1999) but as a small breakout that inflated (Byrnes and Crown, 2001; Patrick et al., 2017). The surface of the tube is composed of uplifted slabs of pāhoehoe lava. Its surface morphology strongly resembles the morphology of a satellite tumulus (Duncan et al., 2004), unlike the Mt. Arcimis lava tube overlaid by lava channels, inflated flows and tumuli (Calvari et al., 2024). These characteristics interrogate us on the way the lava tube at Vesuvius formed and developed.

Inside the lava tube, we observed internal features showing that lava flowed within the lava tube from north to south. Stalactites formed by remelting of the ceiling by hot gases indicate a prolonged lava flowage into the tube. The multiple layers of wall lining also indicate that the lava filled and drained the tube several times (Calvari and Pinkerton, 1999), possibly feeding secondary flows and vents. In addition, wall lining thickness increases from the outer to the innermost portions of the lava tube, testifying an increase in the viscosity and thus a change in the rheological behaviour of the lava flowing inside the lava tube. The last wall lining shows that the lava tube drained suddenly while the wall lining was still plastic allowing it to detach from the wall and roll down on itself to form rolls on the lava tube floor and small spiky horizontal stalactites on the wall. These internal features showed the evolution of the conditions inside the lava tube, its formation and development.

An interpretation of the mechanism that formed the lava tube is in Fig. 13. (1) Initially, a small lava flow of a few tens of meters emplaced. The outer part cooled rapidly and formed a crust, while the internal part stayed hot. The emplaced lava flow was soon under compressive forces as its front and sides cooled down and solidified. (2) The lava flow inflated and the cooled surface crust started to lift. Fractures appeared in the cooled crust forming slabs of pāhoehoe lava. (3) A sustained lava supply allowed the support and consolidation of the fractured roof. (4) The lava tube emptied partially or completely coating the walls and ceiling with lava. (5) The supply of lava increased, and the lava tube was filled again by lava. This process of emptying and refilling of the lava tube took place multiple times. Every time it emplaced a new layer of lava on the walls and ceiling forming numerous wall linings. Throughout time the rheological properties of the lava changed, increasing its viscosity. (6) After a long-lived activity, the supply of lava stopped, and the lava drained out of the lava tube rapidly, leaving a pāhoehoe flow surface and an empty cavity.

The study of lava tubes is essential to comprehend how lava is transported in lava flows as it affects their distance of emplacement. We described a lava tube that was able to transport lava to a limited

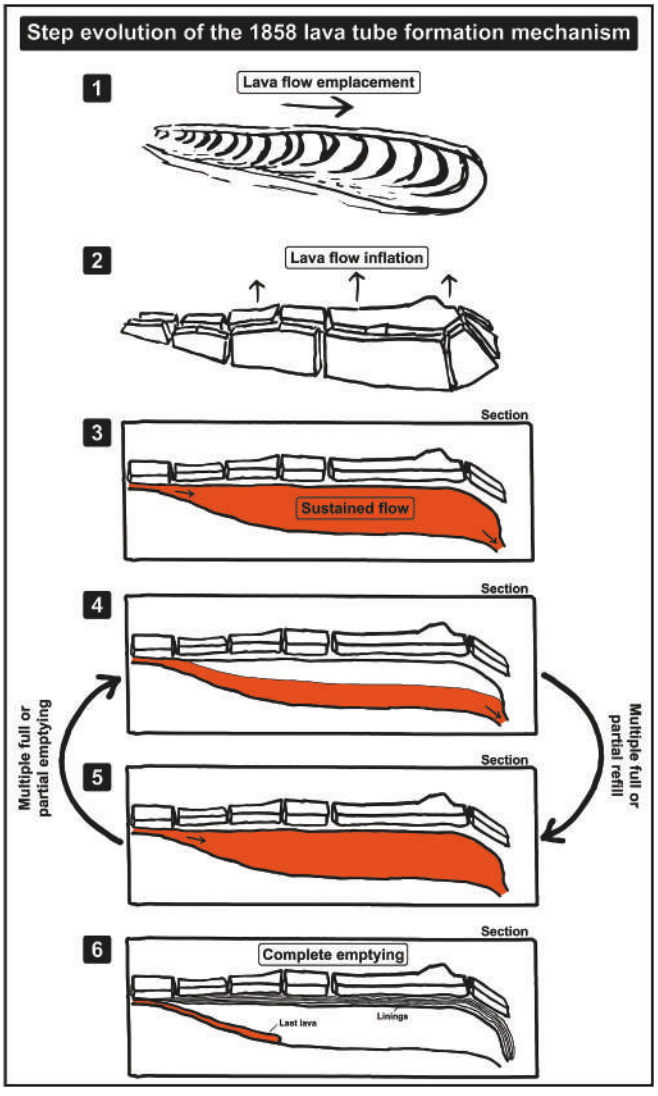

Fig. 13. Step evolution model of the lava tube formation mechanism proposed for tube 3 based on the lava flow inflation process.

distance. However, it must be stressed that this tube is located in the shallowest part of the lava flow field and transported lava for a time long enough to inflate, fill and drain several times. Thus, it could be inferred that larger tubes were present within the lava flow field at a deeper level, feeding the distal margins of the flow field. In addition, it is here worth noting that the volcanic and anthropogenic context in which this lava tube is situated can be even distressed by a limited reach. The highly inhabited flanks of Vesuvius are easily affected in case of lava flow emplacement and the effect of a lava tube as we described in this study can have a significant impact in the reach of damageable areas. Knowing the conditions of lava tube formation and their possible ways of development is fundamental to evaluate and respond adequately to the hazard during or even prior volcanic crises, especially in volcanic areas where constructed and agricultural lands are very close to the eruptive activity.

6. Conclusion

On Vesuvius, the effusive processes are not well studied, given that most of the scientific literature concentrated on the past explosive activity. Our study is one of the first in several decades to focus on the effusive activity and its processes at Vesuvius. This study focuses on the morphological description of the 1858 lava flow field and on the morphologies and mechanisms of formation of lava tubes in the same lava flow field at Vesuvius.

The reconstruction of the development of the 1858 lava flow field at various stages was inferred from historical documents. This reconstruction shows the dynamics of lava flow emplacement which helped understand the formation and development of a lava tube in that lava flow.

Through the digitization and description of this lava tube we showed the presence of lava tubes in volcanic systems in which effusive phases were fed by alkali-rich magmas, different from the typical basaltic magmas. The largest lava tube found in the 1858 lava flow field was re-examined after more than 100 years with the aid of new technologies. The complete 3D scan allowed the study of the lava tube morphology. The presence of internal features such as multiple inner coatings and lava stalactites is evidence that lava flowed into the cavity and therefore that this cavity could be described as a lava tube. Internal features are also important to know and understand the thermal and rheological history of the lava flowing inside the lava tube. The shape in plan view of this lava tube is explained by its origin, namely the emplacement of a pāhoehoe breakout eventually drained. The formation of this lava tube is mainly explained by the process of lava flow inflation (Hon et al., 1994).

In the frame of hazard assessment at Vesuvius, this study is the first step into getting knowledge about the presence and mechanism of formation of lava tubes in the lava flows of Vesuvius. The possible formation of lava tubes, even of limited size, has to be taken into account when forecasting the reach limit of lava flows as it can quickly affect populated and built-up areas.

Author statement

All authors declare that:

- the work described has not been published previously except in the form of a preprint, an abstract, a published lecture, academic thesis or registered report.
- the article is not under consideration for publication elsewhere.
- the article's publication is approved by all authors and tacitly or explicitly by the responsible authorities where the work was carried out.
- if accepted, the article will not be published elsewhere in the same form, in English or in any other language, including electronically without the written consent of the copyright-holder.

CRediT authorship contribution statement

Thomas Lemaire: Writing – review & editing, Writing – original draft, Visualization, Investigation, Formal analysis, Data curation, Conceptualization. **Daniele Morgavi:** Writing – review & editing, Writing – original draft, Supervision, Project administration, Methodology, Investigation, Funding acquisition, Formal analysis, Data curation, Conceptualization. **Paola Petrosino:** Writing – review & editing, Investigation, Conceptualization. **Sonia Calvari:** Writing – review & editing, Investigation, Conceptualization. **Leopoldo Repola:** Writing – review & editing, Data curation. **Lorenzo Esposito:** Writing – review & editing, Data curation. **Diego Di Martire:** Writing – review & editing, Data curation. **Vincenzo Morra:** Writing – review & editing. **Francesco Frondini:** Writing – review & editing.

Declaration of competing interest

The authors declare that they have no known competing financial interests or personal relationships that could have appeared to influence the work reported in this paper.

Data availability

Data will be made available on request.

Acknowledgment

This research was funded by the project "UndersTanding lava tUBe formation and prEServation (TUBES)" PRIN – Bando 2022 PNRR Prot. P2022N55C3 (P.I. D. Morgavi). This research was also partially funded by the Project FIRST-ForecastIng eRuptive activity at Stromboli volcano: Timing, eruptive style, size, intensity, and duration; INGV-Progetto Strategico Dipartimento Vulcani 2019 (Deliberata n. 144/2020). We thank the editor, Shane Cronin, and two anonymous reviewers for their constructive comments. We are thankful to Giovanni Varriale for his help during the 3D survey of the lava tube.

References

Ainsworth, A., Boone Kauffman, J., 2009. Response of native Hawaiian woody species to lava-ignited wildfires in tropical forests and shrublands. In: Van der Valk, A.G. (Ed.), Forest Ecology: Recent Advances in Plant Ecology. Springer, Netherlands, Dordrecht, pp. 197–209. https://doi.org/10.1007/978-90-481-2795-5_15.

Anderson, S.W., Maccolley, S.D., Fink, J.H., Hudson, R.K., 2005. The Development of Fluid Instabilities and Preferred Pathways in Lava Flow Interiors: Insights from Analog Experiments and Fractal Analysis, Special Papers. Geological Society of America, pp. 147–160.

Anderson, S.W., Smrekar, S.E., Stofan, E.R., 2012. Tumulus development on lava flows: insights from observations of active tumuli and analysis of formation models. Bull. Volcanol. 74, 931–946. https://doi.org/10.1007/s00445-012-0576-2.

Arno, V., Principe, C., Rosi, M., Santacroce, R., Sbrana, A., Sheridan, M.F., 1987. Eruptive history. In: Quaderni de "La Ricerca Scientifica,", 114.

Arrighi, S., Principe, C., Rosi, M., 2001. Violent strombolian and subplinian eruptions at Vesuvius during post-1631 activity. Bull. Volcanol. 63, 126–150. https://doi.org/10.1007/s004450100130.

Atkinson, A., Griffin, T.J., Stephenson, P.J., 1975. A major lava tube system from Undara Volcano, North Queensland. Bull. Volcanol. 39, 266–293. https://doi.org/10.1007/BF02597832.

Belkin, H.E., Kilburn, C.R.J., De Vivo, B., 1993. Sampling and major element chemistry of the recent (A.D. 1631–1944) Vesuvius activity. J. Volcanol. Geotherm. Res. 58, 273–290. https://doi.org/10.1016/0377-0273(93)90113-6.

Brown, S.K., Jenkins, S.F., Sparks, R.S.J., Odbert, H., Auker, M.R., 2017. Volcanic fatalities database: analysis of volcanic threat with distance and victim classification. J. Appl. Volcanol. 6, 15. https://doi.org/10.1186/s13617-017-0067-4.

Byrnes, J.M., Crown, D.A., 2001. Relationships between pahoehoe surface units, topography, and lava tubes at Mauna Ulu, Kilauea Volcano, Hawaii. J. Geophys. Res. 106, 2139–2151. https://doi.org/10.1029/2000JB900369.

Calvari, S., Pinkerton, H., 1998. Formation of lava tubes and extensive flow field during the 1991-1993 eruption of Mount Etna. J. Geophys. Res. 103, 27291–27301. https://doi.org/10.1029/97JB03388.

Calvari, S., Pinkerton, H., 1999. Lava tube morphology on Etna and evidence for lava flow emplacement mechanisms. J. Volcanol. Geotherm. Res. 90, 263–280. https://doi.org/10.1016/S0377-0273(99)00024-4.

Calvari, S., Giudice, G., Maugeri, R., Messina, D., Morgavi, D., Miraglia, L., La Spina, A., Spampinato, L., 2024. Complex Lava Tube Networks developed within the 1792-93 Lava Flow Field on Mount Etna (Italy): Insights for hazard assessment. Front. Earth Sci. 12. https://doi.org/10.3389/feart.2024.1448187.

Carracedo, J.C., Troll, V.R., Day, J.M.D., Geiger, H., Aulinas, M., Soler, V., Deegan, F.M., Perez-Torrado, F.J., Gisbert, G., Gazel, E., Rodriguez-Gonzalez, A., Albert, H., 2022. The 2021 eruption of the Cumbre Vieja volcanic ridge on La Palma, Canary Islands. Geol. Today 38, 94–107. https://doi.org/10.1111/gto.12388.

Carta, S., Figari, R., Sartoris, G., Sassi, E., Scandone, R., 1981. A statistical model for vesuvius and its volcanological implications. Bull. Volcanol. 44, 129–151. https://doi.org/10.1007/BF02597700.

Cella, F., Fedi, M., Florio, G., Grimaldi, M., Rapolla, A., 2007. Shallow structure of the Somma–Vesuvius volcano from 3D inversion of gravity data. J. Volcanol. Geotherm. Res. 161, 303–317. https://doi.org/10.1016/j.jvolgeores.2006.12.013.

Chester, D.K., Duncan, A.M., Wetton, P., Wetton, R., 2007. Responses of the Anglo-American military authorities to the eruption of Vesuvius, March 1944. J. Hist. Geogr. 33, 168–196. https://doi.org/10.1016/j.jhg.2006.02.001.

Cioni, R., Santacroce, R., Sbrana, A., 1999. Pyroclastic deposits as a guide for reconstructing the multi-stage evolution of the Somma-Vesuvius Caldera. Bull. Volcanol. 61, 207–222. https://doi.org/10.1007/s004450050272.

Cioni, R., Bertagnini, A., Santacroce, R., Andronico, D., 2008. Explosive activity and eruption scenarios at Somma-Vesuvius (Italy): Towards a new classification scheme. J. Volcanol. Geotherm. Res. 178, 331–346. https://doi.org/10.1016/j.jvolgeores.2008.04.024.

Coltelli, M., Marsella, M., Proietti, C., Scifoni, S., 2012. The case of the 1981 eruption of Mount Etna: an example of very fast moving lava flows. Geochem. Geophys. Geosyst. 13. https://doi.org/10.1029/2011GC003876.

Crown, D.A., Baloga, S.M., 1999. Pahoehoe toe dimensions, morphology, and branching relationships at Mauna Ulu, Kilauea Volcano, Hawai'i. Bull. Volcanol. 61, 288–305. https://doi.org/10.1007/s004450050298.

Cubellis, E., Marturano, A., Pappalardo, L., 2016. The last Vesuvius eruption in March 1944: reconstruction of the eruptive dynamic and its impact on the environment and people through witness reports and volcanological evidence. Nat. Hazards 82, 95–121. https://doi.org/10.1007/s11069-016-2182-7.

Damiano, N., Del Vecchio, U., 2006. Speleogenesi e grotte del Vesuvio. L'appennino meridionale Anno III, Fascicolo II, 170–178.

Del Negro, C., Cappello, A., Bilotta, G., Ganci, G., Hérault, A., Zago, V., 2019. Living at the edge of an active volcano: risk from lava flows on Mt. Etna. GSA Bulletin 132, 1615–1625. https://doi.org/10.1130/B35290.1.

Duncan, A.M., Dibben, C., Chester, D.K., Guest, J.E., 1996. The 1928 Eruption of Mount Etna Volcano, Sicily, and the Destruction of the Town of Mascali. Disasters 20, 1–20. https://doi.org/10.1111/j.1467-7717.1996.tb00511.x.

Duncan, A.M., Guest, J.E., Stofan, E.R., Anderson, S.W., Pinkerton, H., Calvari, S., 2004. Development of tumuli in the medial portion of the 1983 aa flow-field, Mount Etna, Sicily. J. Volcanol. Geotherm. Res. 132, 173–187. https://doi.org/10.1016/S0377-0273(03)00344-5.

Filippi, J.-B., Durand, J., Tulet, P., Bielli, S., 2021. Multiscale Modeling of Convection and Pollutant Transport Associated with Volcanic Eruption and Lava Flow: Application to the April 2007 Eruption of the Piton de la Fournaise (Reunion Island). Atmosphere 12, 507. https://doi.org/10.3390/atmos12040507.

Gemmellaro, M., 1819. Giornale dell'eruzione dell'Etna avvenuta alli 27 Maggio 1819. Stamperia dei regi studi. https://doi.org/10.3931/e-rara-10684.

Gemmellaro, C., 1844. Sulla eruzione dell'Etna del 17 Novembre 1843. Fratelli sciuto, Catania.

Greeley, R., 1971a. Observations of actively forming lava tubes and associated structures. Hawaii No. NASA-TM-X-62014.

Greeley, Ronald, 1971b. Observations of actively forming lava tubes and associated structures, Hawaii. Part II. NASA technical memorandum NASA TM X-62096.

Greeley, R., 1987. The roles of lava tubes in Hawaiian volcanoes. U.S. Geological Survey Professional Paper, Volcanism in Hawaii 1350, 1589–1602.

Guarini, G., Palmieri, L., Scacchi, A., 1855. Eruzione Vesuviane del 1850 e 1855. Naples.

Halliday, W., 2003. Volcanic caves. In: Gunn, J. (Ed.), Encyclopedia of Caves and Karst Science. Routledge, New York, p. 1624. https://doi.org/10.4324/9780203483855.

Hamilton, W., 1772. Observations on Mount Vesuvius. In A Series Of Letters, Addressed to The Royal Society. Cadell, Mount Etna, And Other Volcanos.

Harris, A.J.L., 2015. Chapter 2 - Basaltic Lava Flow Hazard. In: Shroder, J.F., Papale, P. (Eds.), Volcanic Hazards, Risks and Disasters. Elsevier, Boston, pp. 17–46. https://doi.org/10.1016/B978-0-12-396453-3.00002-2. Hazards and Disasters Series.

Harris, A., De Groeve, T., Carn, S., Garel, F., 2016. Risk evaluation, detection and simulation during effusive eruption disasters. SP 426, 1–22. https://doi.org/10.1144/SP426.29.

Hernández, P.A., Padrón, E., Melián, G.V., Pérez, N.M., Padilla, G., Asensio-Ramos, M., Di Nardo, D., Barrancos, J., Pacheco, J.M., Smit, M., 2022. Gas Hazard Assessment at Puerto Naos and La Bombilla Inhabited Areas, Cumbre Vieja Volcano, La Palma, Canary Islands EGU22–7705. https://doi.org/10.5194/egusphere-egu22-7705.

Hon, K.A., Kauahikaua, J., Denlinger, R., Mackay, K., 1994. Emplacement and inflation of pahoehoe sheet flows: Observations and measurements of active lava flows on Kilauea Volcano, Hawaii. GSA Bull. 106, 351–370. https://doi.org/10.1130/0016-7606(1994)106<0351:EAIOPS>2.3.CO;2.

Horn, B.K.P., 1981. Hill shading and the reflectance map. Proc. IEEE 69, 14–47. https://doi.org/10.1109/PROC.1981.11918.

Hróarsson, B., Jónsson, S.S., 1991. Lava Caves in the Hallmundarhraun Lava Flow, Western Iceland. In: Presented at the Proceedings of the 6th International Symposium on Vulcanospeleology, pp. 85–88.

Istituto Geografico Militare, 1908a. Carta topografica del Monte Vesuvio.

Istituto Geografico Militare, 1908b. Il Vesuvio.

Jenkins, S.F., Day, S.J., Faria, B.V.E., Fonseca, J.F.B.D., 2017. Damage from lava flows: insights from the 2014–2015 eruption of Fogo. Cape Verde. J Appl. Volcanol. 6, 6. https://doi.org/10.1186/s13617-017-0057-6.

Johnston-Lavis, H.J., Platania, Sambon, Zezi Lavis, A., 1891. The South Italian Volcanoes. Naples.

Kauahikaua, J., Cashman, K.V., Mattox, T.N., Heliker, C.C., Hon, K.A., Mangan, M.T., Thornber, C.R., 1998. Observations on basaltic lava streams in tubes from Kilauea Volcano, island of Hawai'i. J. Geophys. Res. 103, 27303–27323. https://doi.org/10.1029/97JB03576.

Kereszturi, G., Németh, K., Moufti, M.R., Cappello, A., Murcia, H., Ganci, G., Del Negro, C., Procter, J., Zahran, H.M.A., 2016. Emplacement conditions of the 1256 AD Al-Madinah lava flow field in Harrat Rahat, Kingdom of Saudi Arabia — Insights from surface morphology and lava flow simulations. J. Volcanol. Geotherm. Res. 309, 14–30. https://doi.org/10.1016/j.jvolgeores.2015.11.002.

Keszthelyi, L., 1995. A preliminary thermal budget for lava tubes on the Earth and planets. J. Geophys. Res. 100, 20411–20420. https://doi.org/10.1029/95JB01965.

Le Hon, H., 1866. Carte topographique des laves du Vésuve.

Malladra, A., 1917. Grotta di scolamento lavico negli efflussi vesuviani del 1858. Bolletina della societa dei naturalisti in Napoli XXX (Serie II., Vol.X), 109–124.

Maravigna, C., 1819. Istoria dell'incendio dell'Etna del mese maggio 1819. Pastore.

Marsigli, V., 1832. A Map of Vesuvius.

Mercalli, G., 1881. Natura delle eruzioni dello Stromboli ed in generale dell'attività sismo-vulcanica nelle Eolie.

Mercalli, G., 1884. Notizie sullo stato attuale dei vulcani attivi italiani.

Mercalli, G., 1888. L' isola vulcano e lo Stromboli dal 1886 al 1888.

Mercalli, G., 1889. Le eruzioni dell'Isola Vulcano.

Meredith, E.S., Jenkins, S.F., Hayes, J.L., Deligne, N.I., Lallemant, D., Patrick, M., Neal, C., 2022. Damage assessment for the 2018 lower East Rift Zone lava flows of Kīlauea volcano. Hawai'i. Bull Volcanol 84, 65. https://doi.org/10.1007/s00445-022-01568-2.

Meredith, E.S., Jenkins, S.F., Hayes, J.L., Lallemant, D., Deligne, N.I., Teng, N.R.X., 2024. Lava flow impacts on the built environment: insights from a new global dataset. J. Appl. Volcanol. 13, 1. https://doi.org/10.1186/s13617-023-00140-7.

Ollier, C.D., Brown, M.C., 1965. Lava caves of Victoria. Bull Volcanol 28, 215–229. https://doi.org/10.1007/BF02596928.

Palmieri, L., 1859. Cronaca del Vesuvio dal 1855 al 1859. Annali dell'osservatorio Vesuviano 46–80.

Palmieri, L., Capocci, E., Giordano, G., Schiavoni, F., Cappa, R., Guiscardi, G., 1862. Intorno all'incendio del Vesuvio : cominciato il dì 8 dicembre 1861. Universita, Naples, Stamperia della R.

Paolillo, A., Principe, C., Bisson, M., Gianardi, R., Giordano, D., La Felice, S., 2016. Volcanology of the Southwestern sector of Vesuvius volcano, Italy. J. Maps 12, 425–440. https://doi.org/10.1080/17445647.2016.1234982.

Patrick, M., Orr, T., Fisher, G., Trusdell, F., Kauahikaua, J., 2017. Thermal mapping of a pāhoehoe lava flow, Kīlauea Volcano. J. Volcanol. Geotherm. Res. 332, 71–87. https://doi.org/10.1016/j.jvolgeores.2016.12.007.

Pesaresi, C., Marta, M., Palagiano, C., Scandone, R., 2008. The evaluation of "social risk" due to volcanic eruptions of Vesuvius. Nat. Hazards 47, 229–243. https://doi.org/10.1007/s11069-008-9214-x.

Peterson, D.W., Holcomb, R.T., Tilling, R.I., Christiansen, R.L., 1994. Development of lava tubes in the light of observations at Mauna Ulu, Kilauea Volcano, Hawaii. Bull Volcanol 56, 343–360. https://doi.org/10.1007/BF00326461.

Petrosino, P., Alberico, I., Caiazzo, S., Piaz, A.D., Lirer, L., Scandone, R., 2004. Volcanic risk and evolution of the territorial system in the volcanic areas of Campania. Acta Vulcanol. 16, 163–178.

Phillips, J., 1869. Vesuvius.

Pigonati, A., 1767. Descrizione delle ultime eruzioni del Monte Vesuvio. Stamperia Simoniana, Naples.

Rossi, M.J., Gudmundsson, A., 1996. The morphology and formation of flow-lobe tumuli on Icelandic shield volcanoes. J. Volcanol. Geotherm. Res. 72, 291–308. https://doi.org/10.1016/0377-0273(96)00014-5.

Roth, J., 1857. Der Vesuv und die umgebung von Neapel, eine monographie.

Santacroce, R., Sbrana, A., 2003. Carta geologica del Vesuvio.

Santacroce, R., Cioni, R., Marianelli, P., Sbrana, A., Sulpizio, R., Zanchetta, G., Donahue, D.J., Joron, J.L., 2008. Age and whole rock–glass compositions of proximal pyroclastics from the major explosive eruptions of Somma-Vesuvius: a review as a tool for distal tephrostratigraphy. J. Volcanol. Geotherm. Res., Expl. Volcanism Central Mediterranean area during the late Quaternary - linking sources and distal archives 177, 1–18. https://doi.org/10.1016/j.jvolgeores.2008.06.009.

Sauro, F., Pozzobon, R., Massironi, M., De Berardinis, P., Santagata, T., De Waele, J., 2020. Lava tubes on Earth, Moon and Mars: a review on their size and morphology revealed by comparative planetology. Earth Sci. Rev. 209, 103288. https://doi.org/10.1016/j.earscirev.2020.103288.

Scandone, R., Giacomelli, L., Gasparini, P., 1993. Mount Vesuvius: 2000 years of volcanological observations. J. Volcanol. Geotherm. Res. 58, 5–25. https://doi.org/10.1016/0377-0273(93)90099-D.

Swanson, D.A., 1973. Pahoehoe Flows from the 1969–1971 Mauna Ulu Eruption, Kilauea Volcano. Hawaii. GSA Bulletin 84, 615–626. https://doi.org/10.1130/0016-7606(1973)84<615:PFFTMU>2.0.CO;2.

Tarquini, S., Isola, I., Favalli, M., Battistini, A., Dotta, G., 2023. TINITALY, a digital elevation model of Italy with a 10 meters cell size (Version 1.1). Doi:10.13127/TINITALY/1.1.

Tomasi, I., Massironi, M., Meyzen, C., Pozzobon, R., Sauro, F., Penasa, L., Santagata, T., Tonello, M., Gómez, G., Martínez-Frías, J., 2022. Inception and Evolution of La Corona Lava Tube System (Lanzarote, Canary Islands, Spain). J. Geophys. Res. Solid Earth 127. https://doi.org/10.1029/2022JB024056.

Trigila, R., De Benedetti, A.A., 1993. Petrogenesis of Vesuvius historical lavas constrained by Pearce element ratios analysis and experimental phase equilibria. J. Volcanol. Geotherm. Res. 58, 315–343. https://doi.org/10.1016/0377-0273(93)90115-8.

Unknow author, Monte Vesuvio. https://doi.org/10.3931/e-rara-40988.

Vasconez, F.J., Ramón, P., Hernandez, S., Hidalgo, S., Bernard, B., Ruiz, M., Alvarado, A., Femina, P.L., Ruiz, G., 2018. The different characteristics of the recent eruptions of Fernandina and Sierra Negra volcanoes (Galápagos, Ecuador). Volcanica 1, 127–133. https://doi.org/10.30909/vol.01.02.127133.

Ventura, G., Vilardo, G., 2008. Emplacement mechanism of gravity flows inferred from high resolution Lidar data: The 1944 Somma–Vesuvius lava flow (Italy). Geomorphology 95, 223–235. https://doi.org/10.1016/j.geomorph.2007.06.005.

Villemant, B., Trigila, R., DeVivo, B., 1993. Geochemistry of Vesuvius volcanics during 1631–1944 period. J. Volcanol. Geotherm. Res. 58, 291–313. https://doi.org/10.1016/0377-0273(93)90114-7.

Wadge, G., 1978. Effusion rate and the shape of aa lava flow-fields on Mount Etna. Geology 6, 503–506. https://doi.org/10.1130/0091-7613(1978)6<503:ERATSO>2.0.CO;2.

Wadge, G., 1981. The variation of magma discharge during basaltic eruptions. J. Volcanol. Geotherm. Res. 11, 139–168. https://doi.org/10.1016/0377-0273(81)90020-2.

Walker, G.P.L., 1991. Structure, and origin by injection of lava under surface crust, of tumuli, lava rises, lava-rise pits, and lava-inflation clefts in Hawaii. Bull. Volcanol. 53, 546–558. https://doi.org/10.1007/BF00298155.

Witter, J.B., Harris, A.J.L., 2007. Field measurements of heat loss from skylights and lava tube systems. J. Geophys. Res. 112. https://doi.org/10.1029/2005JB003800, 2005JB003800.

Zuccarello, F., Bilotta, G., Cappello, A., Ganci, G., 2022. Effusion rates on Mt., Etna and Their Influence on Lava Flow Hazard Assessment. Remote Sens. 14, 1366. https://doi.org/10.3390/rs14061366.